

RADIATION LOAD FROM RADIATIVE BHABHA SCATTERING IN THE FCC-ee EXPERIMENTAL INSERTIONS

A. Frasca^{1*}, H. Burkhardt, A. Lechner, G. Lerner, J. Mańczak, CERN, Geneva, Switzerland

M. Boscolo, A. Ciarma, INFN, Frascati, Italy

C. Welsch¹, N. Kumar¹, Cockcroft Institute, Warrington, UK

¹also at University of Liverpool, Liverpool, UK

Abstract

The lepton Future Circular Collider (FCC-ee) at CERN provides e^+e^- collisions at four interaction points (IPs) along a 91 km ring, with beam energies spanning from 45.6 GeV (Z pole) to 182.5 GeV ($t\bar{t}$ threshold). The radiation showers produced by these collisions can reach sensitive components of the surrounding machine elements, possibly affecting their performance and lifetime. This contribution examines the case of radiative Bhabha scattering, which generates off-momentum beam particles that can be lost downstream of the IPs. Some losses occur already at the superconducting final focusing quadrupoles (FFQs), where they can cause quenches and degradation of the coil materials. In this work, the Monte Carlo code FLUKA is used to study the impact of radiative Bhabha in the experimental insertion regions of FCC-ee. The radiation load in the FFQs and the radiation levels in the nearby tunnel and machine elements are simulated for the Z-pole and $t\bar{t}$ operational modes. For the FFQs, a tungsten shielding layer with optimized thickness is proposed to mitigate the radiation load in the magnet coils.

INTRODUCTION

The Future Circular Collider (FCC) is a staged project studying the realization of next colliders at CERN for the post-LHC era. It proposes the construction of a 90.7 km underground tunnel, where first a lepton collider, the FCC-ee [1], and then a hadron collider, the FCC-hh [2], could be built. The FCC-ee, expected to start operating in the 2040s, will serve as an electroweak, Higgs and top factory, providing e^+e^- collisions at center-of-mass energies ranging from Z pole (91.2 GeV) to $t\bar{t}$ threshold (365 GeV). The FCC-ee will feature high peak luminosities of $1.45 \times 10^{36} \text{ cm}^{-2} \text{ s}^{-1}$ and $1.41 \times 10^{34} \text{ cm}^{-2} \text{ s}^{-1}$ at Z pole and $t\bar{t}$, respectively.

Given the high beam energies and luminosities, the radiation showers triggered by the collision products can significantly affect the machine elements in the experimental insertions, compromising their efficiencies and lifetime. One of the processes with the highest cross section is radiative Bhabha (RB) scattering, $e^+e^- \rightarrow e^+e^-\gamma$, i.e., a Bhabha scattering with the emission of one or more photons. The radiating e^+ or e^- can lose up to the near-totality of their kinetic energy, thereby exceeding the energy acceptance range of the machine, and resulting in their impact on the vacuum chamber downstream of the interaction point (IP). The lower magnetic rigidity of these particles also increases their sus-

ceptibility to beam-beam kicks at the IP, modifying their angular distribution at the IP.

Lower-energy RB particles are lost already in the final focus quadrupoles (FFQs). The current final focus design foresees a doublet of NbTi superconducting canted-cosine-theta quadrupoles, QC1 and QC2, composed of three and two segments, respectively [3]. Their high field gradients lead to localized losses that expose them to potential magnet quenching and radiation damage. Moreover, with $L^* = 2.2 \text{ m}$, QC1 is housed in a liquid-He cryostat entirely inside the experiment detector, making its safe operation even more critical. By contrast, higher-energy RB particles may be lost over the next few hundred meters downstream, while those within the energy acceptance of the machine can remain in orbit, most likely contributing to the beam halo. While the warm magnets in the ring do not pose quench risks, the radiation levels produced by these losses may be a concern for the distributed machine equipment, like cables and electronics.

Estimating the radiation load on the FFQs and tunnel radiation levels is crucial during the design phase, as it helps identifying mitigation strategies where necessary. In this work we use FLUKA [4–6] to quantify the power density and the total ionizing dose (TID) in the superconducting coils of the FFQs, as well as the radiation environment in FCC-ee experimental insertions, resulting from RB scattering at the IP. The effects of a tungsten shielding layer surrounding QC1 beam pipe on the calculated quantities are also analyzed, supporting its installation as a magnet protection measure. The results are shown for the operational mode with the highest luminosity, Z pole, and the highest beam energy, $t\bar{t}$.

SIMULATION SETUP

FLUKA is a Monte Carlo code designed to simulate particle transport and interactions in matter within user-defined 3D geometries, utilizing state-of-the-art physics models.

A representative geometry of one side of FCC-ee experimental insertion region, similar to that in [7], has been modeled in FLUKA (Fig. 1). It extends up to $\approx 725 \text{ m}$ from the IP, including the outgoing e^+ beamline, the incoming e^- beamline, and the concrete tunnel surrounded by soil. The tunnel is divided into three straight segments to approximate its curvature and varying cross section. The FFQ models, based on the current design, feature a water-cooled stainless steel beam pipe, implemented with a 1.4 mm-thick layer of water between two 0.8 mm-thick layers of steel. The magnet, separated from the beam pipe by 0.2 mm of vacuum, is simplified using four alternating layers: 2 mm-thick Al and

* alessandro.frasca@cern.ch

Table 1: Power deposition in FFQ layers (mW) due to RB scattering at Z pole and $t\bar{t}$ simulated with FLUKA. For QC1 segments at Z pole, values in parentheses represent power deposition with 2 mm-thick W shielding in place.

Magnet	QC1R1		QC1R2		QC1R3		QC2R1		QC2R2	
	Z pole	$t\bar{t}$	Z pole	$t\bar{t}$	Z pole	$t\bar{t}$	Z pole	$t\bar{t}$	Z pole	$t\bar{t}$
Gradient [T/m]	-40.8	-97.3	-29.5	-82.7	-19.4	-94.3	39.4	14.8	-0.00632	76.5
Al (I)	14 (3.7)	0.051	130 (26)	0.72	280 (52)	2.7	60	2.4	5.3	0.53
Coils (I)	33 (9.8)	0.15	300 (69)	1.9	650 (140)	6.6	150	5.8	12	1.3
Al (II)	5.7 (1.9)	0.029	52 (14)	0.36	110 (28)	1.1	30	1.0	2.1	0.26
Coils (II)	14 (5.4)	0.073	130 (39)	0.86	270 (81)	2.7	81	2.6	5.2	0.69
Total	66 (21)	0.30	610 (150)	3.8	1300 (300)	13	320	13	25	2.8

4 mm-thick coil material, for a total thickness of 12 mm. The equivalent coil material is a compound of Al, NbTi, and Cu, with a density of 5.09 g cm^{-3} . The beam pipe in QC1 and QC2 has an inner radius of 1.5 cm and 2 cm, respectively. For the rest of the beamline, a 2 mm-thick copper beam pipe with a 3-cm radius aperture is assumed. Horizontal winglets are added to the outgoing beam pipe. The FLUKA models of room-temperature magnets are implemented with an iron yoke and copper coils. The simulation is based on optics v24.4 and the current baseline interaction region layout. It features a 30 mrad crossing angle and local solenoid compensation, implemented through a 3D magnetic field map including a 2-T detector solenoid, a -5-T compensation solenoid, and a screening solenoid around the FFQs.

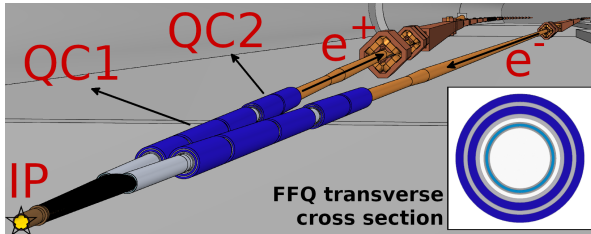


Figure 1: FLUKA model of FCC-ee experimental insertion.

The samples of RB particles are generated with BB-Brem [8] and GUINEA-PIG++ [9]. BBBrem is a Monte Carlo generator of RB events in the forward direction, programmed to calculate the cross section of the process at a given center-of-mass energy, with cutoffs on the minimum energy of the radiated photon and on the minimum momentum transfer. The first cutoff sets an upper limit on the energy spectrum of the radiating particles. The second defines the maximum interaction distance and reflects the finite interaction range experienced by e^+ or e^- in a bunch due to the electromagnetic fields of the other particles. This effect was significant at the Large Electron-Positron (LEP) collider, where the measured cross section was reproduced with BBBrem when bunch dimensions were taken into account [8]. Consequently, a cutoff of 10_y (40.1 nm at Z pole and 43.6 nm at $t\bar{t}$) was employed for all the RB samples used in this work. The particle-in-cell code GUINEA-PIG++ is used to apply smearing and beam-beam effects to the events generated with BBBrem in the center-of-mass frame, assuming gaussian beams with nominal parameters.

FINAL FOCUS

Preliminary simulations have shown that approximately 99.6% at Z pole and 99.8% at $t\bar{t}$ of the RB particles lost within the final focus have less than half the nominal beam energy. Therefore, RB samples with a photon energy cutoff at 50% of the nominal beam energy have been generated to study the effects on the FFQs with improved statistics and efficiency. The resulting RB cross sections are 18.45 mb and 18.57 mb at Z pole and $t\bar{t}$, respectively. The power deposition in the different layers of QC1 and QC2 downstream of the IP due to RB e^+ is reported in Table 1, ranging from fractions to hundreds of mW per segment. The magnet QC1 is more exposed than QC2, with a maximum deposition of 1.3 W in QC1R3 at Z pole. The power deposition at $t\bar{t}$ is significantly lower than at Z pole, due to the lower luminosity.

The total power figures are not concerning, as they can be managed by the cryogenic system, but the local peak values of power density and TID in the coils are more critical. This is due to an asymmetric loss pattern that results from the combination of the lower magnetic rigidity of RB particles, asymmetric beam-beam effects, and the strong horizontal defocusing fields of QC1. The horizontal angular distributions simulated by GUINEA-PIG++ show an asymmetric tail at negative angles (toward the internal side of the collider), leading to an average negative offset in the horizontal position of the particles at QC1 entrance. This effect is more pronounced at Z pole, where a horizontal offset of -1.0 mm is observed, compared to -0.2 mm at $t\bar{t}$. Consequently, most RB particles are defocused toward and lost on the internal side of the magnet. Figure 2 shows the peak TID accumulated over one operational year ($\approx 10^7$ s) and

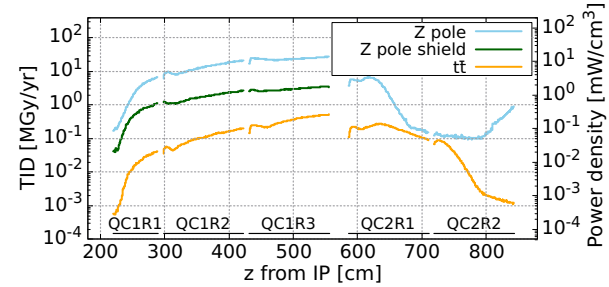


Figure 2: Peak values of TID and power density in FFQ coils due to RB scattering as simulated with FLUKA.

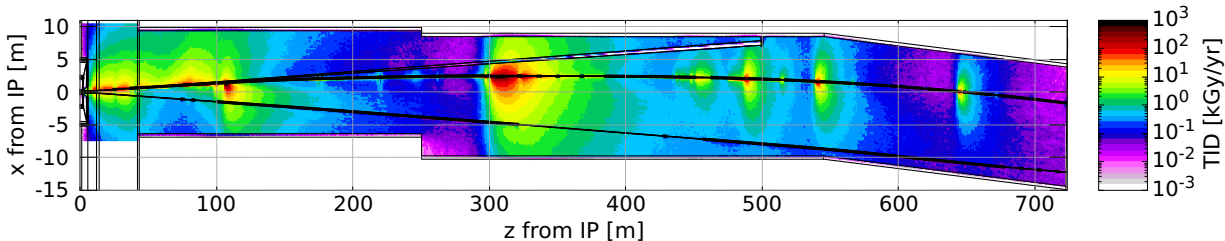


Figure 3: Top view of annual TID in experimental insertion region from RB scattering at Z pole as simulated with FLUKA.

the peak instantaneous power density in the FFQ superconducting coils, both evaluated at peak luminosity. The plot highlights QC1R3 at Z pole as the most critical case, where the TID reaches 28 MGy yr^{-1} and the power density peaks at 14 mW cm^{-3} . These values exceed acceptable limits for both quenching and radiation damage, necessitating an internal shielding layer in the magnet design. Tungsten is a natural choice due to its high density, ensuring effective shielding over short distances [10]. FLUKA simulations including a W layer around QC1 with a thickness of 2 mm demonstrate a significant reduction in the power absorbed by QC1 at Z pole (Table 1), ranging from around 68% to 77%. Local peak values (Fig. 2) show even greater improvements. The proposed shield lowers peak values by about 87%, bringing the TID to 3.6 MGy yr^{-1} and power density to 1.8 mW cm^{-3} . These levels align with LHC cold-magnet design limits of 30 MGy [11] over the full lifetime and 4 mW cm^{-3} [12], even with a design margin to account for uncertainties or additional radiation sources.

TUNNEL RADIATION LEVELS

Preparatory studies revealed that only a few RB particles with energy above 93% of the nominal beam energy were lost within 725 m downstream of the IP: fewer than 0.03% at Z pole and 0.01% at $t\bar{t}$. Accordingly, RB samples with a photon energy cutoff at 7% of the nominal beam energy were produced to study their effect on the tunnel radiation levels. The RB cross sections are 81.99 mb and 82.54 mb, at Z pole and $t\bar{t}$, respectively. A top view of the annual TID at beamline height (average for y in ± 20 cm) for Z-pole operation is shown in Fig. 3. Several radiation hotspots, ranging from 10 kGy yr^{-1} to 100 kGy yr^{-1} , appear along the beamline, particularly in regions with reduced material budget around the vacuum chamber, such as drifts and magnets accommodating the beamstrahlung extraction line [13]. The exact hotspot locations are determined by the RB loss map, which is strongly influenced by the machine optics. A similar loss pattern is observed at $t\bar{t}$, though tunnel dose levels are lower by two orders of magnitude due to the reduced luminosity. At Z pole, synchrotron radiation (SR) has a critical energy of only a few tens of keV and does not induce particle showers, thus RB is the dominant radiation source in the experimental insertion region. In contrast, at $t\bar{t}$, SR dominates the radiation environment, with a critical energy of approximately 1 MeV, making the RB contribution negligible [7]. Once the optics is well established, shielding

solutions shall be explored to mitigate the RB hotspots, taking into account the different energy of the lost particles compared to the case of SR.

In addition to electromagnetic showers, RB losses generate neutrons via photonuclear reactions, whose spectra in air below the beamline are shown in Fig. 4 for both Z-pole and $t\bar{t}$ operation at different distances from the IP. Given the high energies of RB particles, the energy of these neutrons can also extend up to the GeV scale, unlike those produced by beamstrahlung radiation at Z pole or SR at $t\bar{t}$, which do not exceed the MeV scale. The impact of these additional GeV-level neutrons on electronics is expected to be more severe, and it needs to be considered when choosing the placement of instrumentation.

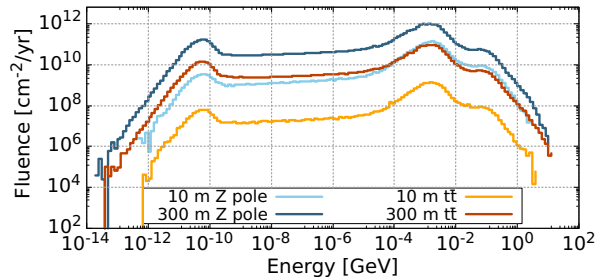


Figure 4: Neutron fluence produced by RB scattering downstream of the IP at Z pole and $t\bar{t}$ simulated with FLUKA.

CONCLUSION

The impact of RB on the superconducting FFQs and on the tunnel radiation levels has been studied with FLUKA in the FCC-ee experimental insertion region, with input samples from BBBrem and GUINEA-PIG++. While the total power deposition in QC1 and QC2 at the Z pole is about 2.3 W, the asymmetric RB loss pattern leads to excessive local peak values of power density and TID in the coils. Maximum peaks of 14 mW cm^{-3} and 28 MGy yr^{-1} are found in QC1R3. Simulations indicate that a 2 mm-thick tungsten shielding around QC1 can mitigate these effects, reducing the peak values to 1.8 mW cm^{-3} and 3.6 MGy yr^{-1} . At $t\bar{t}$, the lower luminosity results in values two orders of magnitude lower. The RB losses dominate the radiation environment only at Z pole, with hotspots up to 100 kGy yr^{-1} , whereas at $t\bar{t}$ SR prevails. Additionally, photonuclear reactions generate GeV-level neutrons in both operational modes, potentially affecting electronics and other machine equipment.

REFERENCES

- [1] M. Benedikt *et al.*, “FCC-ee: The Lepton Collider: Future Circular Collider Conceptual Design Report Volume 2”, CERN, Geneva, Switzerland, Rep. CERN-ACC-2018-0057, Dec. 2018. doi:10.1140/epjst/e2019-900045-4
- [2] M. Benedikt *et al.*, “FCC-hh: The Hadron Collider: Future Circular Collider Conceptual Design Report Volume 3”, CERN, Geneva, Switzerland, Rep. CERN-ACC-2018-0058, Dec. 2018. doi:10.1140/epjst/e2019-900087-0
- [3] A. Thabuis, M. Koratzinos, G. Kirby, M. Liebsch, and C. Petrone, “The first superconducting final focus quadrupole prototype of the FCC-ee study”, in *Proc. IPAC’24*, Nashville, TN, USA, pp. 2851–2853, May 2024. doi:10.18429/JACoW-IPAC2024-WEPS65
- [4] FLUKA website, <https://fluka.cern/>.
- [5] G. Battistoni *et al.*, “Overview of the FLUKA code”, *Ann. Nucl. Energy*, vol. 82, pp. 10–18, 2015. doi:10.1016/j.anucene.2014.11.007
- [6] C. Ahdida *et al.*, “New Capabilities of the FLUKA Multi-Purpose Code”, *Front. Phys.*, vol. 9, 2022. doi:10.3389/fphy.2021.788253
- [7] A. Frasca *et al.*, “Energy deposition and radiation level studies for the FCC-ee experimental insertions”, in *Proc. IPAC’24*, Nashville, TN, USA, pp. 1152–1155, May 2024. doi:10.18429/JACoW-IPAC2024-TUPC66
- [8] R. Kleiss and H. Burkhardt, “BBBREM — Monte Carlo simulation of radiative Bhabha scattering in the very forward direction”, *Comput. Phys. Commun.*, vol. 81, pp. 372–380, 1994. doi:10.1016/0010-4655(94)90085-X
- [9] C. Rimbault *et al.*, “GUINEA-PIG++: An Upgraded Version of the Linear Collider Beam-Beam Interaction Simulation Code GUINEA-PIG”, in *Proc. PAC’07*, Albuquerque, NM, USA, pp. 2728–2730, Jun 2007. doi:10.1016/0010-4655(94)90085-X
- [10] L. S. Esposito, F. Cerutti, and E. Todesco, “FLUKA Energy Deposition Studies for the HL-LHC”, in *Proc. IPAC’13*, Shanghai, China, pp. 1379–1381, May 2013. <https://jacow.org/IPAC2013/papers/TUPFI021.pdf>
- [11] G. Arduini *et al.*, “LHC Triplet Task Force Report”, CERN, Geneva, Switzerland, Rep. CERN-ACC-2023-0004, Nov. 2023.
- [12] N. V. Mokhov, I. L. Rakhno, I. S. Tropin, F. Cerutti, L. S. Esposito, and A. Lechner, “Energy deposition studies for the high-luminosity large hadron collider inner triplet magnets”, *Phys. Rev. ST Accel. Beams*, vol. 18, May 2015. doi:10.1103/PhysRevSTAB.18.051001
- [13] C. J. Eriksson, “Magnet design for beamstrahlung photons extraction line”, presented at FCC week 2023, London, June 2023.